Electronic Supplementary Material (ESI) for Dalton Transactions.
This journal is © The Royal Society of Chemistry 2019

Supplementary Information for

MMCT excited state of localized mixed valence Cyanido - Bridged Ru^{II}-$Ru_2^{III,III}$-Ru^{II} complex

Shao-Dong Su, [ab] Xiao-Quan Zhu, [a] Lin-Tao Zhang, [ab] Yu-Ying Yang, [ab] Yue-Hong Wen, [a] Xin-Tao Wu, [a] Song-Qiu Yang *,[c] and Tian-Lu Sheng, *,[a]

[a] State Key Laboratory of Structural Chemistry, Fujian Institute of Research on the Structure of Matter, Chinese Academy of Sciences, Fuzhou 350002, People's Republic of China

[b] University of the Chinese Academy of Sciences, Beijing 100049, People's Republic of China

[c] State Key Laboratory of Molecular Reaction Dynamics, Dalian Institute of Chemical Physics, Chinese Academy of Sciences, Dalian 116023, People's Republic of China

Table of Contents

1. Crystallographic data

Table S1: Crystallographic data and a summary of the structural refinements for complexes **1-2**

Table S2: Crystallographic data and a summary of the structural refinements for (Me-Cp)(dppe)-$Ru^{II}CN$ and Cp^*Ru^{II}(dppe)CN

Table S3: Selected bond lengths and angles of (Me-Cp)(dppe)$Ru^{II}CN$ and Cp^*Ru^{II}(dppe)CN

2. Electronic absorption spectra

Figure S1-S2: UV/Vis/NIR spectra of complexes $CpRu^{II}$(dppe)CN and Cp^*Ru^{II}(dppe)CN in CH_2Cl_2 solution

Figure S3-S4: UV/Vis/NIR spectra of complex **1** in DMF and acetonitrile solution

Figure S5: UV/Vis/NIR spectra of complex **2** in different solvents

Table S4: Gaussian peak fitting data of complexes **1** and **2.**

3. The IR spectra

Figure S6: The IR spectra of $CpRu^{II}$(dppe)CN and Cp^*Ru^{II}(dppe)CN

4. TD-DFT calculations

Table S5: Summary of TD-DFT calculations

5. Transient absorption studies

Figure S7-S8: Femtosecond time-resolved transient absorption spectra of complex **2** and $Ru_2(DMBA)_4(NO_3)_2$ with λ_{pump}= 750 nm.

Figure S9: Femtosecond time-resolved transient absorption spectra of complex **2** with λ_{pump}= 616 nm.

Figure S10: UV/Vis/NIR spectra of $[Cp^*Ru^{III}(dppe)Cl]^+$ and $[CpRu^{III}(dppe)(CH_3CN)]^+$

Figure S11: Life-time fitting results for the complexes **1** and **2**

Table S6: Excited State Lifetimes of Some Cyano-Bridged Complexes

6. Electrochemical Properties

Figure S12: Cyclic voltammograms properties of complex **1** and **2**

7. References

1. Crystallographic data

Table S1. Crystallographic data and a summary of the structural refinements for complexes **1-2**

Complex	1·0.6CH_2Cl_2	2
Formula	$C_{100.6}H_{103.2}Cl_{1.2}F_{12}N_{10}P_6Ru_4$	$C_{110}H_{122}C_{l0}F_{12}N10P_6Ru_4$
Color	Deep Purple	Deep Blue
Crystal system	Monoclinic	Cubic
Space group	C 2/c	I 2 3
a (A)	28.640(6)	32.2832(16)
b (A)	22.121(4)	32.2832(16)
c (A)	21.051(5)	32.2832(16)
alpha (deg.)	90	90
beta (deg.)	121.458(3)	90
gamma (deg.)	90	90
Volume(A^3)	11377(4)	33646(5)
Z	4	12
Formula weight	2312.97	2402.27
Density(cal.)(Mg /m^3)	1.350	1.423
μ(mm^-1)	0.699	0.684
T(K)	100	100
Theta range (deg.)	2.171 to 24.999	2.185 to 25.000
Independent reflections	10004	9844
Observed Reflection	7933	9525
Reflections measured	38575	143314
Final R indices (obs.)	R1 = 0.0564 wR2 = 0.1165	R1 = 0.0616 wR2 = 0.1537
R indices (all)	R1 = 0.0690 wR2 = 0.1226	R1 = 0.0638 wR2 = 0.1571
Goodness-of-fit	0.998	1.005

$R_1 = \Sigma(||F_0| - |F_c||)/\Sigma|F_0|$;

$wR_2 = [\Sigma w(|F_0^2| - |F_c^2|)^2/\Sigma w|F_0^2|^2]^{1/2}$

Table S2. Crystallographic data and a summary of the structural refinements for (Me-Cp)(dppe)Ru^{II}CN and Cp*Ru^{II}(dppe)CN

Complex	(Me-Cp)(dppe)Ru^{II}CN·CH_2Cl_2	Cp*Ru^{II}(dppe)CN
formula	C_{34} H_{33} Cl_2 N P_2 Ru	C_{37} H_{39} N P_2 Ru
Color	yellow	yellow
Crystal system	Monoclinic	Monoclinic
Space group	P 21/n	P 21/c
a (A)	13.1304(14)	11.154(5)
b (A)	9.1192(9)	17.875(7)
c (A)	26.004(3)	16.895(9)
alpha (deg.)	90	90
beta (deg.)	90.552(11)	108.837(8)
gamma (deg.)	90	90
Volume(A^3)	3113.6(6)	3188(3)
Z	4	4
Formula weight	689.52	660.70
Density(cal.)(Mg/m^3)	1.471	1.377
μ(mm^-1)	0.803	0.618
Temperature(K)	100(2)	100(2)
Theta range (deg.)	2.367 to 27.476	2.248 to 27.601
Reflections measured	28070	27403
Independent reflections	7090 (Rint = 0.0423)	7279 (Rint = 0.0509)
Observed Reflection	6079 (I > 2\s(I))	5758 (I > 2\s(I))
Final R indices (obs.)	R1 = 0.0391, wR2 = 0.1064	R1 = 0.0313, wR2 = 0.0603
R indices (all)	R1 = 0.0456, wR2 = 0.1246	R1 = 0.0413, wR2 = 0.0627
Goodness-of-fit	1.085	1.001

$R_1 = \Sigma(||F_0| - |F_c||)/\Sigma|F_0|$;

$wR_2 = [\Sigma w(|F_0^2| - |F_c^2|)^2/\Sigma w|F_0^2|^2]^{1/2}$

Table S3. Selected bond lengths and angles of (Me-Cp)(dppe)Ru^{II}CN and Cp*RuII(dppe)CN

(Me-Cp)(dppe)Ru^{II}CN	Cp*Ru^{II}(dppe)CN
Ru(1)-C(1) 2.005(3)	Ru(1)-C(1) 2.010(3)
Ru(1)-P(1) 2.2750(8)	Ru(1)-P(1) 2.2717(11)
Ru(1)-P(2) 2.2652(8)	Ru(1)-P(2) 2.2762(10)
Ru(1)-C(2) 2.253(3)	Ru(1)-C(28) 2.280(2)
Ru(1)-C(3) 2.233(3)	Ru(1)-C(29) 2.259(2)
Ru(1)-C(4) 2.239(3)	Ru(1)-C(30) 2.237(2)
Ru(1)-C(5) 2.256(3)	Ru(1)-C(31) 2.229(2)
Ru(1)-C(7) 2.266(3)	Ru(1)-C(32) 2.276(2)
N(1)-C(1) 1.151(4)	N(1)-C(1) 1.155(3)
N(1)-C(1)-Ru(1) 177.2(3)	N(1)-C(1)-Ru(1) 176.4(2)
P(1)-Ru(1)-P(2) 82.55(3)	P(1)-Ru(1)-P(2) 82.63(4)

2. Electronic absorption spectroscopy

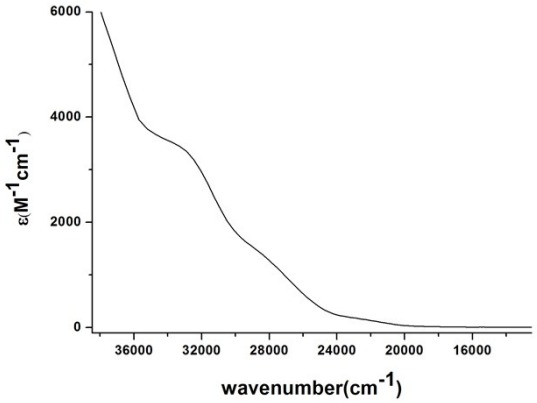

Figure S1. UV/Vis/NIR spectra of complex $CpRu^{II}(dppe)CN$ in CH_2Cl_2 solution

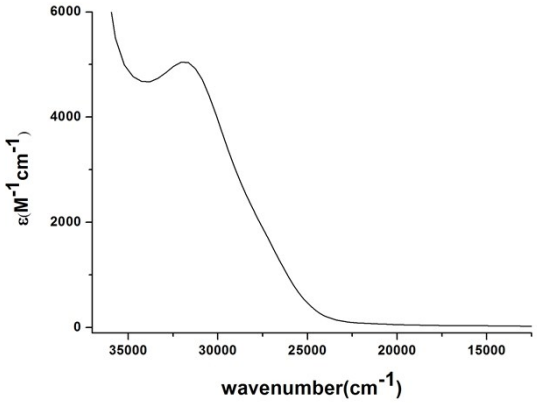

Figure S2.UV/Vis/NIR spectra of complex $Cp^*Ru^{II}(dppe)CN$ in CH_2Cl_2 solution

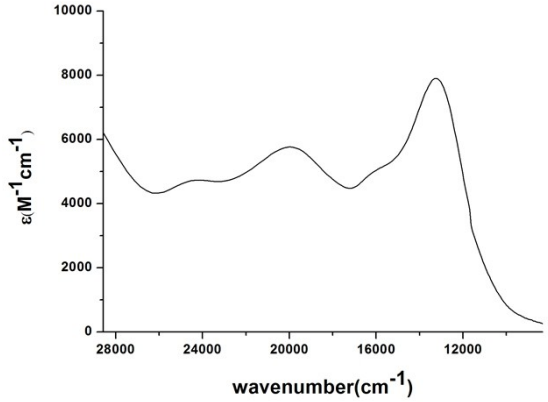

Figure S3. UV/Vis/NIR spectra of complex **1** in DMF solution

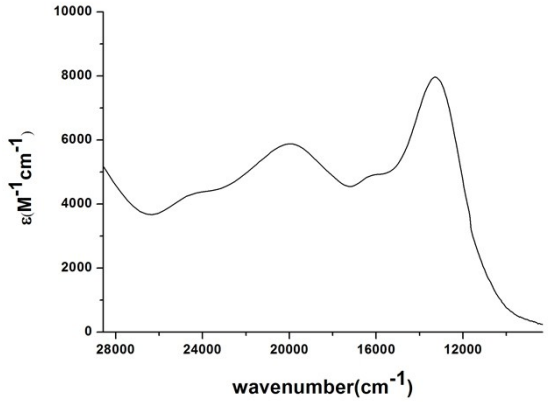

Figure S4.UV/Vis/NIR spectra of complex **1** in acetonitrile solution

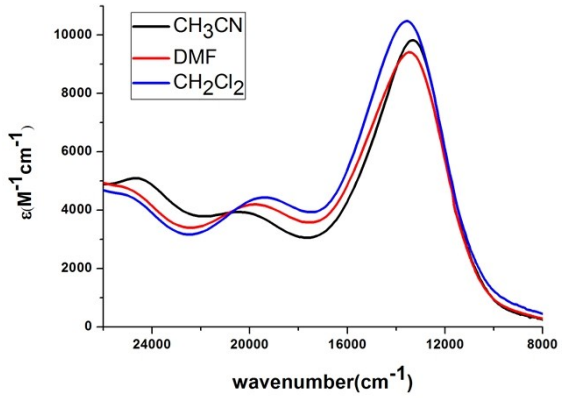

Figure S5. UV/Vis/NIR spectra of complex **2** in different solvents

Table S4. Gaussian peak fitting data of complexes **1** and **2**.

ν_{max} (ε_{max}, FWHM) [cm^{-1}($M^{-1}cm^{-1}$, cm^{-1})]					
	Peak 1	Peak 2	Peak 3	Peak 4	Peak 5
1	23125	20301	18531	15625	13082
	(3326,3797)	(3416,3539)	(2876,3492)	(5124,3281)	(6697,2531)
2	24687	20351	17891	14238	13203
	(4143,4375)	(3020,3281)	(2879,3906)	(5197,3984)	(5758,3242)

3. The IR spectra

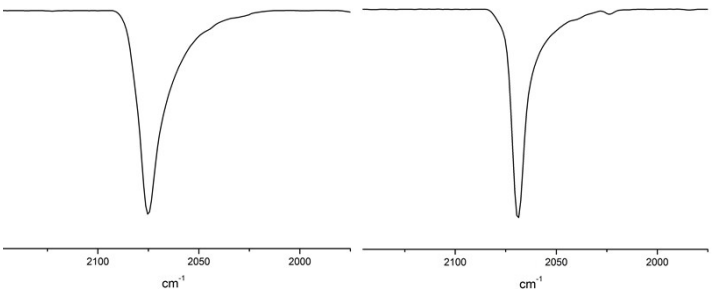

Figure S6. The IR spectra of $CpRu^{II}(dppe)CN$ (left, 2075 cm^{-1}) and $Cp^{*}Ru^{II}(dppe)CN$ (right, 2069 cm^{-1})

4. TD-DFT calculations

Table S5. Predicted MMCT absorption bands, main orbital transitions, oscillator strengths (f) of complexes **1-2** calculated by the TD-DFT M06/lanl2dz level **.**

Complex	MMCT band (nm)	Energy (eV)	orbital transition	oscillator strengths (f)
1	**662.67**	**1.8710**	**424B→427B (0.74632)**	**0.0490**
2	**804.81**	**1.5405**	**464B→467B (0.71385)**	**0.0266**

5. Transient absorption studies

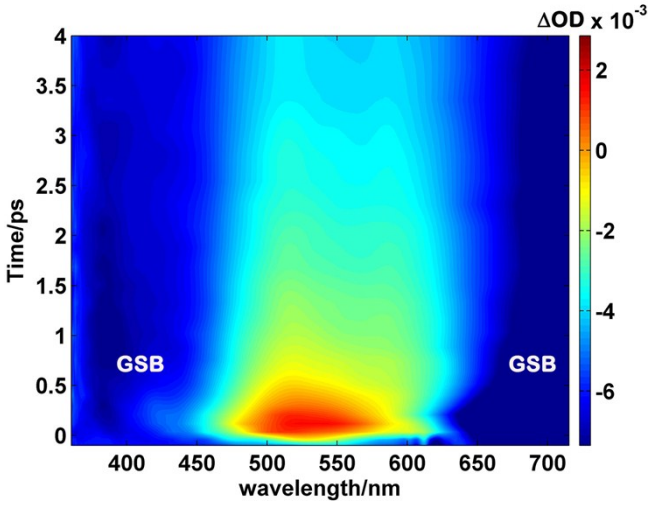

Figure S7. Femtosecond time-resolved transient absorption spectra of $Ru_2(DMBA)_4(NO_3)_2$ with λ_{pump}= 750 nm.

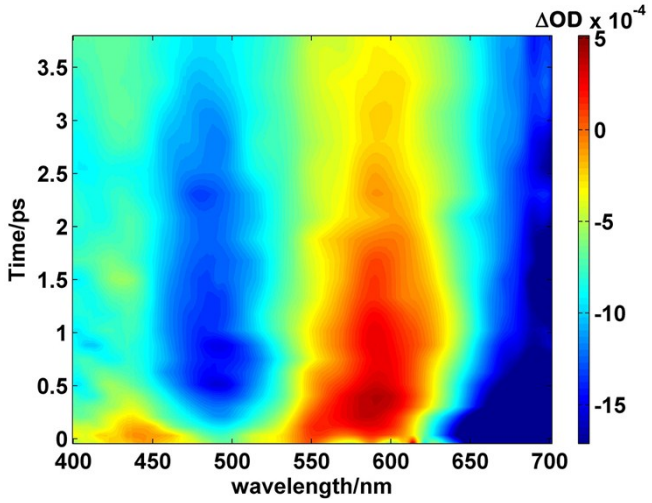

Figure S8. Femtosecond time-resolved transient absorption spectra of complex **2** with λ_{pump}= 750 nm.

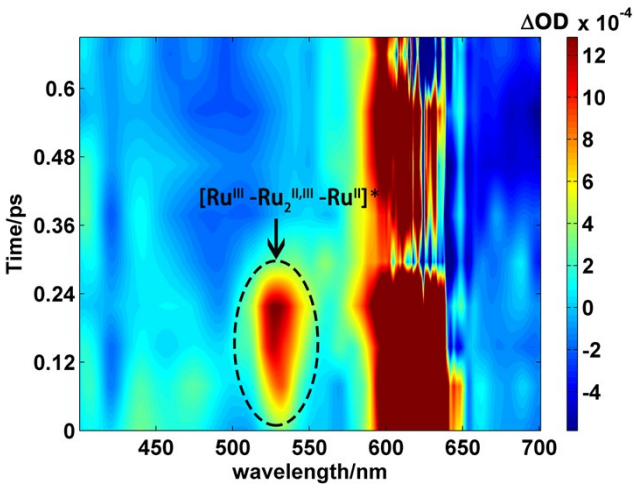

Figure S9. Femtosecond time-resolved transient absorption spectra of complex **2** with λ_{pump}= 616 nm.

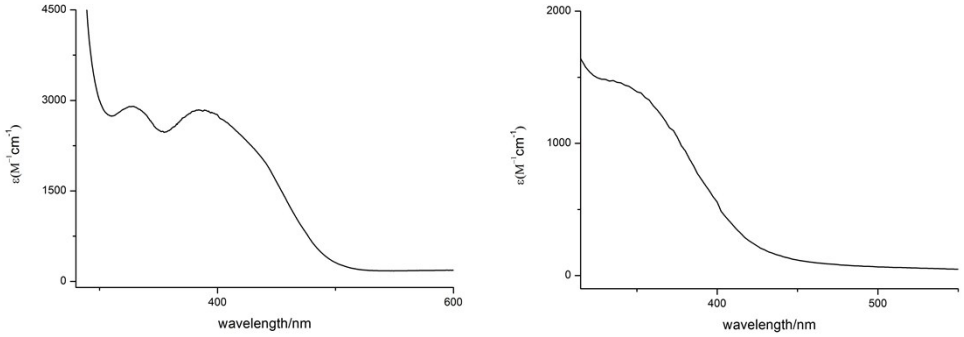

Figure S10. UV/Vis/NIR spectra of $[Cp^*Ru^{III}(dppe)Cl]^+$ (left) and $[CpRu^{III}(dppe)(CH_3CN)]^+$ (right)

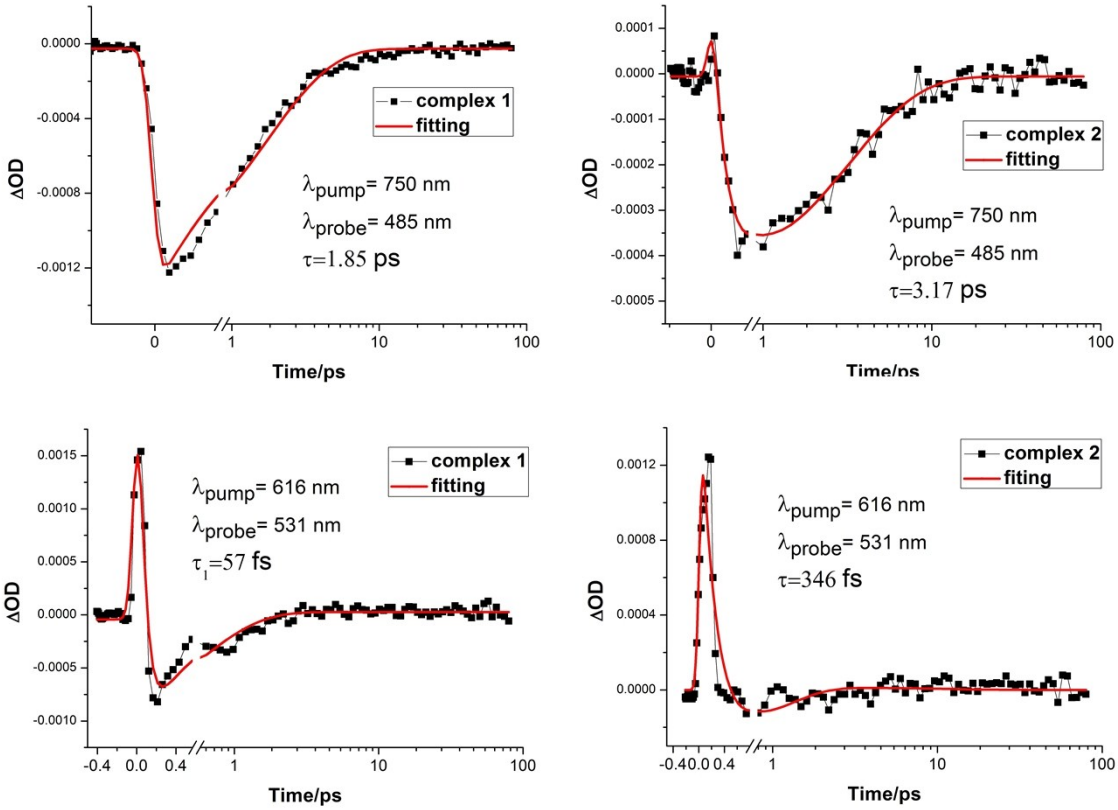

Figure S11. Life-time fitting results for the complexes **1** and **2**

Table S6. Some excited state lifetimes reported

complex	lifetime (τ) (fs)	ref
Ru^{II}-NC-Ru^{III}	85	**1**
Ru^{II}-NC-Fe^{III}	89	**2**
Os^{II}-NC-Os^{III}	<500	**3**
Co^{II}-NC-Fe^{III}	750	**4**

6. Electrochemical Properties

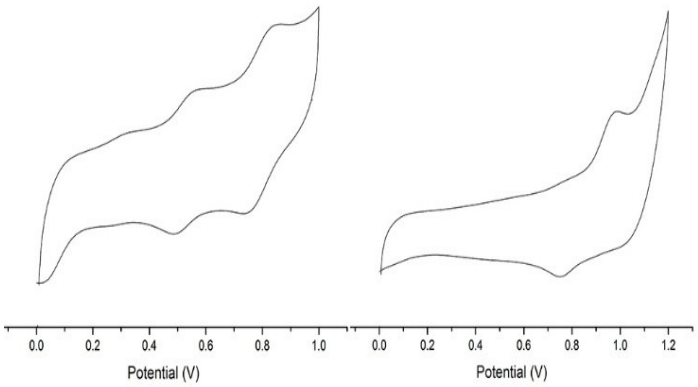

Figure S12. Cyclic voltammograms of **1** (left) and **2** (right) in the 0.10M CH_2Cl_2 solution of n-Bu_4NPF_6 at a scan rate of 100 mV/s (Ag/AgCl reference electrode)

The cyclic voltammograms of complexes **1-2** were measured in dichloromethane respectively. As shown in Figure S12, complex **1** exhibits oxidation processes at 0.52 and 0.85 V. Compared with the cyclic voltammograms of the precursor complexes $Ru_2(DMBA)_4(NO_3)_2$ and $CpRu^{II}(dppe)CN$, the first oxidation process at 0.52 V is likely belong to the oxidation of the diruthenium component $Ru_2^{5+/6+}$, whereas the second one at 0.85 V can be assigned to the oxidation process of $CpRu^{II}(dppe)CN$. For complex **2**, a quite irreversible electrochemical property can be observed. The irreversible oxidation process (0.98v) may be assigned to the oxidation of the $Cp^*Ru^{II}(dppe)CN$ (0.79v).

7. References

[1] a) K. Tominaga, D. V. Kliner, A. E. Johnson, N. E. Levinger and P. F. Barbara, *J. Chem. Phys.*1993, **98**, 1228-1243; b) P. J. Reid, C. Silva, P. F. Barbara, L. Karki and J. T. Hupp, *J. Phys. Chem.*1995, **99**, 2609-2616.

[2] G. C. Walker, P. F. Barbara, S.K. Doorn, Y.H. Dong and J. T. Hupp, *J. Phys. Chem.* 1991, **95**, 5712-5715.

[3] S. K. Doorn, R. B. Dyer, P.O. Stoutland and W. H. Woodruff, *J. Am. Chem. Soc.* 1993, **115**, 6398-6405.

[4] B. P. Macpherson, P. V. Bernhardt, A. Hauser, S. Pages and E. Vauthey, *Inorg. Chem.* 2005, **44**, 5530−5536.